Geochemical Perspectives Letters

River chemistry reveals a large decrease in dolomite abundance across the Phanerozoic

J.M. Husson[1*], L.A. Coogan[1]

OPEN ACCESS

https://doi.org/10.7185/geochemlet.2316

Abstract

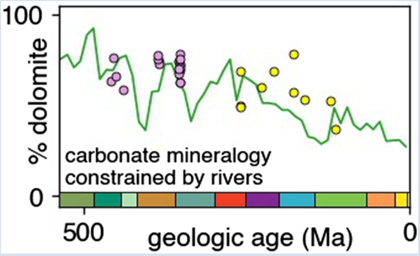

The abundance of dolomite in ancient carbonate sediments, and its apparent rarity today, has important implications for the coupled Ca-Mg-C-cycles in seawater and global climate. Despite its importance, there are large differences between published records of dolomite abundance *vs.* geologic age, mainly due to complexities in adequately sampling heterogeneous bedrock. We overcome this issue by using dissolved Mg^{2+} and Ca^{2+} measurements in rivers draining carbonate-bearing bedrock. Because rivers weather broad areas, this approach integrates the geochemical composition of much larger volumes of carbonate compared to sample based methods. The average Mg/(Ca + Mg) molar ratio in rivers declines with decreasing bedrock age, from 0.44 at ~485 million year old (Ma) to 0.14 at ~5 Ma, suggesting a decreasing percentage of dolomite in carbonate sequences across the Phanerozoic Eon. These data are hard to reconcile with any model that relies only upon oscillatory drivers to explain the dolomite abundance record, such as sea level or episodic expansions of ocean anoxia, and have important implications for the oceanic Mg cycle.

Received 31 October 2022 | Accepted 20 April 2023 | Published 26 May 2023

Introduction

A truism in sedimentary geology is that dolomite, $(Ca_{0.5},Mg_{0.5})CO_3$, is more common in ancient carbonates compared to younger sequences (Daly, 1909). Dolomite is also a rare precipitate from the modern ocean, despite seawater being highly dolomite supersaturated (Land, 1998). These two observations form the core of "the dolomite problem" (*e.g.*, Holland and Zimmermann, 2000; Petrash *et al.*, 2017). While much research addresses the origin of dolomite, there is still no consensus on how its abundance varies with geologic age. Some time series show a monotonic decrease in the dolomite to calcite ratio from the beginning of the Phanerozoic towards today (Vinogradov and Ronov, 1956; Schmoker *et al.*, 1985). Others are stationary and show large oscillations around a Phanerozoic mean (Given and Wilkinson, 1987; Li *et al.*, 2021). Better constraints on dolomite abundance across Earth history are crucial for understanding its broader implications. If older rocks systematically contain more dolomite than younger ones, then carbonate weathering delivers more Mg to the oceans than can be balanced by carbonate burial, requiring an additional sink(s). The dolomite problem thus affects the cycling of Ca-Mg-C in the Earth system, with important implications for global climate (*e.g.*, Arvidson *et al.*, 2011).

Previous dolomite abundance records have used Mg/Ca ratios in carbonate samples (Vinogradov and Ronov, 1956; Given and Wilkinson, 1987), or descriptions of limestone and dolostone in sedimentary sequences (Schmoker *et al.*, 1985; Li *et al.*, 2021). A major challenge to these methods is that the samples or units must be representative of a much larger volume of carbonate rock. Description based syntheses have the added challenge of converting qualitative field descriptions to quantitative percentages of carbonate mineralogies. To circumvent these problems, we measure dolomite abundance in the rock record using dissolved Mg^{2+} and Ca^{2+} concentrations in rivers. Owing to its greater efficiency compared to silicate weathering, carbonate weathering globally delivers ~84 % of the total riverine flux of Mg^{2+} and Ca^{2+} (Gaillardet *et al.*, 1999). Therefore, it is reasonable to expect that rivers draining carbonate bedrock would have a similar Mg/Ca to average carbonate in the catchment, and detailed studies of watersheds with ~30–70 % carbonate outcrop in Slovenia (Szramek *et al.*, 2011) and Michigan (Williams *et al.*, 2007) support this assertion. In our compiled record, in catchments that drain carbonate-bearing bedrock, the average Mg/(Ca + Mg) molar ratio of rivers (referred to here as F_{Mg}) declines monotonically with decreasing bedrock age. This signal is interpreted as providing the most robust published record of the decrease in dolomite to calcite ratio over the Phanerozoic.

Methods

Measurements of dissolved Ca^{2+}, Mg^{2+}, Na^+, K^+, Cl^-, pH, $CO_{2(aq)}$ and alkalinity on filtered river water samples were compiled from the USGS National Water Information System (NWIS) and the Global River Chemistry (GLORICH; Hartmann *et al.*, 2014) databases. Geologic maps stored in Macrostrat (Peters *et al.*, 2018) were used to constrain the bedrock geology that directly underlies each stream measurement station (Supplementary Information). An upper and lower bedrock age was assigned based on the chronostratigraphic age bin assigned to the underlying geologic unit. The bedrock for each river sampling site was

1. School of Earth and Ocean Sciences, University of Victoria, Victoria, BC, V8W2Y2 Canada
* Corresponding author (email: jhusson@uvic.ca)

designated a 'station fraction carbonate' value (f_{stn}), calculated as the number of listed carbonate lithologies divided by the total number of listed lithologies. For example, if a measurement station sits on a geologic unit that is described as "limestone, sandstone and siltstone," its f_{stn} value would be 0.33. In all, the total area of the carbonate containing map units that underlie stream stations is 3.39 x 10^6 km^2, which is 10 % of the total continental area estimated to be covered by carbonate or mixed carbonate-siliciclastic sediments (33.4 x 10^6 km^2; Hartmann and Moosdorf, 2012).

As a test whether this surface lithology determination was robust, we used Macrostrat to describe the bedrock geology of entire watersheds that contain NWIS stations. This approach utilised the USGS National Watershed Boundary Dataset (WBD) that demarcates the U.S.A. into separate watersheds (Supplementary Information). Using geological map data, an area-weighted 'watershed fraction carbonate' value (f_{ws}) was calculated for each watershed that contains a NWIS station. For example, if a watershed is composed of two mapped units of equal area (one igneous, and one carbonate-siliciclastic), its f_{ws} would be 0.25. An upper and lower age for the watershed's bedrock was determined by the area-weighted average of the upper and lower ages of the carbonate containing map units. Both f_{stn} and f_{ws} are derived from qualitative text descriptions from 174 different geologic maps (Supplementary Information). Therefore, these 'fraction carbonate' parameters do not quantify carbonate abundance in bedrock precisely, but simply provide a filter that we can use to separate the dataset into carbonate-richer and carbonate-poorer subsets, to test the role this difference plays in controlling the resulting river chemistry.

Results

Population averages and standard deviations of F_{Mg} for each station were calculated to avoid overweighting of sites with multiple measurements. Station-averaged F_{Mg} was then included if 1σ is less than 10 % to ensure reproducibility of F_{Mg} at the station level. Locations of these NWIS and GLORICH stations are shown in Figure 1.

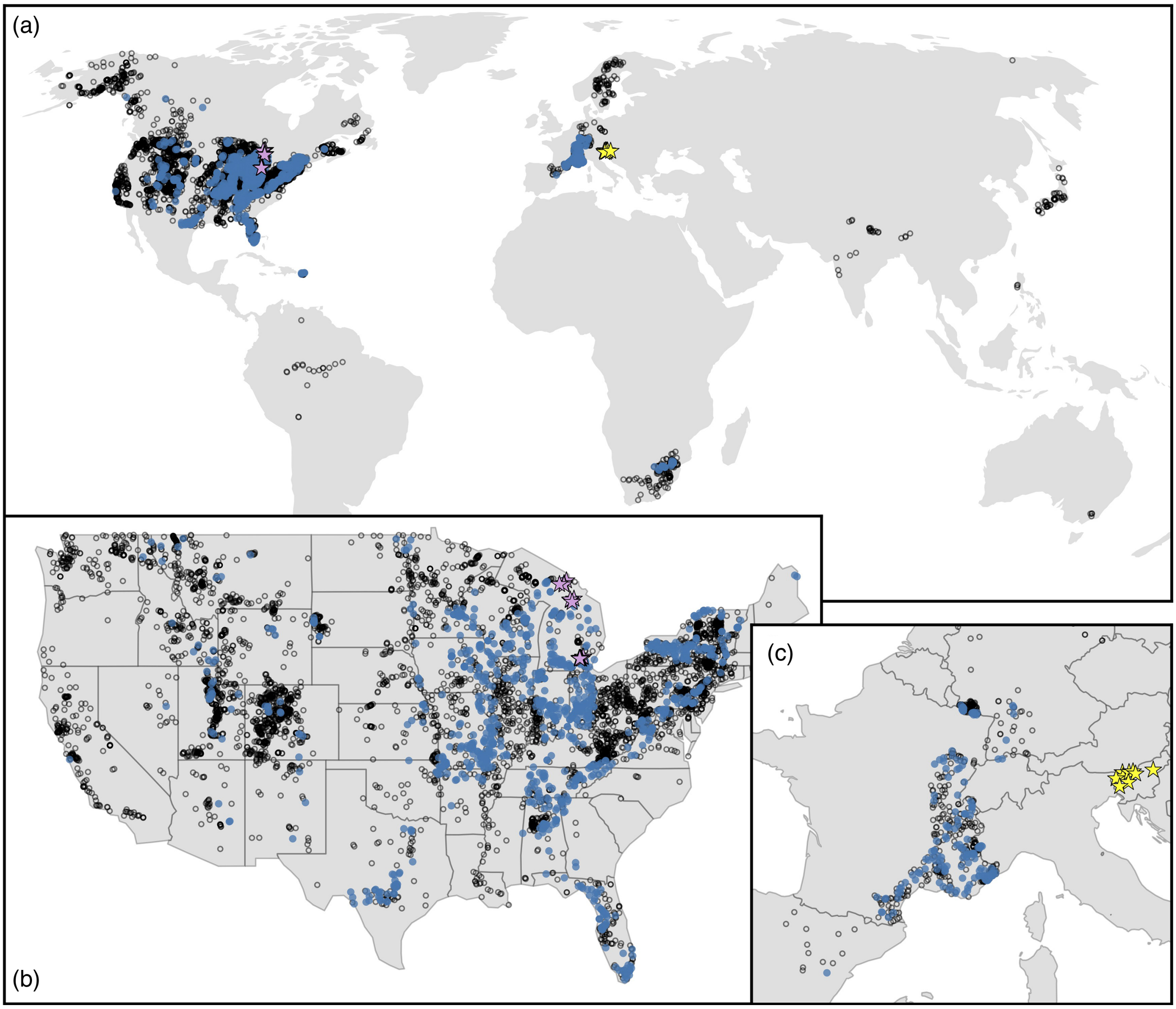

Figure 1 **(a)** Map showing locations of river stations plotted in Figure 2. All localities are included in Figure 2a, whereas blue dots are carbonate-draining rivers included in Figure 2b or c. In **(b)** and **(c)**, inset maps of the contiguous U.S.A. and western Europe, respectively, are shown. Also plotted are rivers in Michigan (purple stars; Williams *et al.*, 2007) and Slovenia (yellow stars; Szramek *et al.*, 2011) draining catchments with ~30–70 % carbonate outcrop.

Bedrock age *vs.* station-averaged F_{Mg} shows no secular trend (Fig. 2a), a result more clearly seen when the data are shown as age binned averages. Before binning, the dataset was sampled *via* 10,000 Monte Carlo trials, wherein each station's F_{Mg} is drawn from a normal distribution defined by its mean and standard deviation, and bedrock age is drawn from a uniform distribution defined by each station's top and bottom age. Average F_{Mg} was then calculated on this re-sampled dataset for evenly spaced 10 million year (Myr) bins that span the Phanerozoic. These age binned F_{Mg} values have a mean value of 0.32, similar to the mean of all station averages (0.33).

When data are only included from rivers that drain carbonate containing bedrock, the time series look dramatically different (Fig. 2b, c). We took three steps to identify these rivers (blue dots; Fig. 1). First, to reduce the influence of silicate weathering, samples with molar ratios of K/(Ca + Mg) and Na/(Ca + Mg) above 0.061 and 0.36, respectively, were excluded. These upper limits are based upon the K^+ and Na^+ content of NWIS stream samples from 134 watersheds with $f_{ws} \geq 0.9$, where carbonate weathering is expected to dominate (Fig. S-1). While these selected upper limits are somewhat arbitrary, there is no correlation between F_{Mg} and K^+ or Na^+ (Fig. S-2); therefore, picking different limits would not change the overall distribution of F_{Mg}.

Second, river water samples were only included if their ratio of HCO_3^- to ($Mg^{2+} + Ca^{2+}$) is between 1 and 2, which are the predicted end member ratios for calcite and dolomite weathering *via* sulfuric acid and carbonic acid, respectively (Szramek *et al.*, 2011). Therefore, a HCO_3/(Ca + Mg) ratio within this range is evidence that the Mg^{2+} and Ca^{2+} within a sample are derived from dissolved carbonate minerals. For each water sample, we calculated [HCO_3^-] and calcite saturation state, Ω, using the Python toolbox PyCO2SYS 1.8.1 (Humphreys *et al.*, 2022), using either measured pH and $CO_{2(aq)}$ (148,621 samples) or measured pH and alkalinity (58,983 samples) to solve the carbonate system. Of these samples, 80 % have a HCO_3/(Ca + Mg) ratio consistent with a carbonate weathering source.

Third, and lastly, the relative number of described carbonate lithologies found in geologic maps were used to select rivers that drain carbonate containing bedrock, determined either at the station level ($f_{stn} \geq 0.33$; Fig. 2b) or at the watershed level ($f_{ws} \geq 0.33$; Fig. 2c). These cut offs are similar to the low end of carbonate richness in watersheds that were studied in detail for carbonate and dolomite weathering (Williams *et al.*, 2007; Szramek *et al.*, 2011), although our results are not sensitive to the exact cut off used (see below).

In the f_{stn} filtered subset, a clear secular change in F_{Mg} is observed, with a decrease from ~0.44 to 0.14 from the beginning to end of the Phanerozoic. To test whether the approach to filtering the data using the fraction of carbonate rock in weathered bedrock impacts the result, a range of f_{stn} limits were used, along with the K/(Ca + Mg), Na/(Ca + Mg) and HCO_3/(Ca + Mg) filtering. These experiments produce similar time series with similar Phanerozoic declines in F_{Mg} (Figs. S-3, S-4). Comparable results are found if using the same filtering parameters except excluding the HCO_3/(Ca + Mg) filter (Fig. S-5). These sensitivity tests suggest that our results are robust to the uncertainties in how the fraction of carbonate in the bedrock is used to filter the river chemistry. A similar decline in F_{Mg} over the Phanerozoic is seen with the f_{ws} filtered subset, although this subset is only from NWIS, and lacks data between 260 and 120 Ma (Fig. 2c). Watershed bedrock age and average F_{Mg} (*per* sampling site) were also calculated for the well characterised, carbonate weathering Slovenian and Michigan watersheds (Williams *et al.*, 2007; Szramek *et al.*, 2011). These data are not included in the age binned F_{Mg} values in Figure 2c, but they follow the same trend. In summary, regardless of the exact filtering approach used, the observation that Mg/(Ca + Mg) ratio of river water declines steadily with decreasing bedrock age is a clear and reproducible signal from these data.

Discussion

Where carbonate weathering is the predominant source of dissolved Ca^{2+} and Mg^{2+}, the most important control on river F_{Mg} is the relative abundance of calcite and dolomite in the catchment's bedrock (Williams *et al.*, 2007; Szramek *et al.*, 2011). Factors that can alter F_{Mg} after weathering include calcite precipitation (increase F_{Mg} through Ca^{2+} removal) or pollution from $CaCl_2$ in road salts (decrease F_{Mg} through Ca^{2+} addition). No discernible relationship exists between Ω and F_{Mg} (Fig. S-6 and colour coding in Fig. 2b, c) or between Cl/(Ca + Mg) and F_{Mg} (Fig. S-7) and there is no obvious reason why either process should correlate with bedrock age. Thus, we consider the systematic decline in F_{Mg} across the Phanerozoic (Fig. 2b, c) to reflect systematic changes in bedrock carbonate mineralogy. A simple mixing model is used to convert the f_{stn} filtered F_{Mg} record (squares in Fig. 2b) to mole fraction dolomite in carbonate bedrock (Fig. 3). This model assumes that carbonates are composed of either dolomite (47.4 mol % $MgCO_3$, the average for Phanerozoic dolomites from Manche and Kaczmarek, 2021) or low-Mg calcite (2 mol % $MgCO_3$; Morse and Mackenzie, 1990). Aragonite and high-Mg calcite, both important constituents of modern shallow water carbonate sediments, are assumed to undergo open system recrystallisation to low-Mg calcite during early diagenesis and lithification (Morse and Mackenzie, 1990).

River-derived dolomite abundances are compared with previous Phanerozoic compilations of dolomite fraction in Figure 3. The record of Vinogradov and Ronov (1956) is from a region not covered by the river data (the Russian platform) and is the largest previously published dataset (8,847 sample analyses from 198 formations). Dolomite abundances from this record are similar to, or slightly lower than, ours for most of the Phanerozoic, but show a much lower fraction of dolomite in the Cretaceous and Cenozoic. The Russian dataset is much sparser in these time periods, containing only 5 % of the studied formations and 3 % of samples. By contrast, 15 % of Phanerozoic river stations, representing 10 % of the river sample analyses, are of these ages. In contrast to its similarity to the Russian time series, river-derived fraction dolomite (Fig. 3) is strikingly different to the records from both Given and Wilkinson (1987) and Li *et al.* (2021). The lack of systematic fluctuations in dolomite fraction in the river record, unlike those proposed by these authors, and much higher early Phanerozoic dolomite abundance than suggested by Li *et al.* (2021), raises questions about their models of sea level (Given and Wilkinson, 1987) or ocean redox (Li *et al.*, 2021) controlling dolomite formation.

The record of the fraction of dolomite in carbonate successions determined here is based on those carbonates exposed on the continents and hence is largely composed of shelf carbonates. However, there was shift of a substantial amount of carbonate deposition from continental margins to the abyss in the mid-Mesozoic (Wilkinson and Walker, 1989). Because abyssal carbonates are dominantly calcite, this shift means that the change in the dolomite fraction recorded by any study of continental rocks (including this one) must provide an underestimate of the global change in the fraction of dolomite in carbonate rocks formed since the mid-Mesozoic.

If the average Mg/Ca of carbonates has dropped systematically over the Phanerozoic, this has important implications

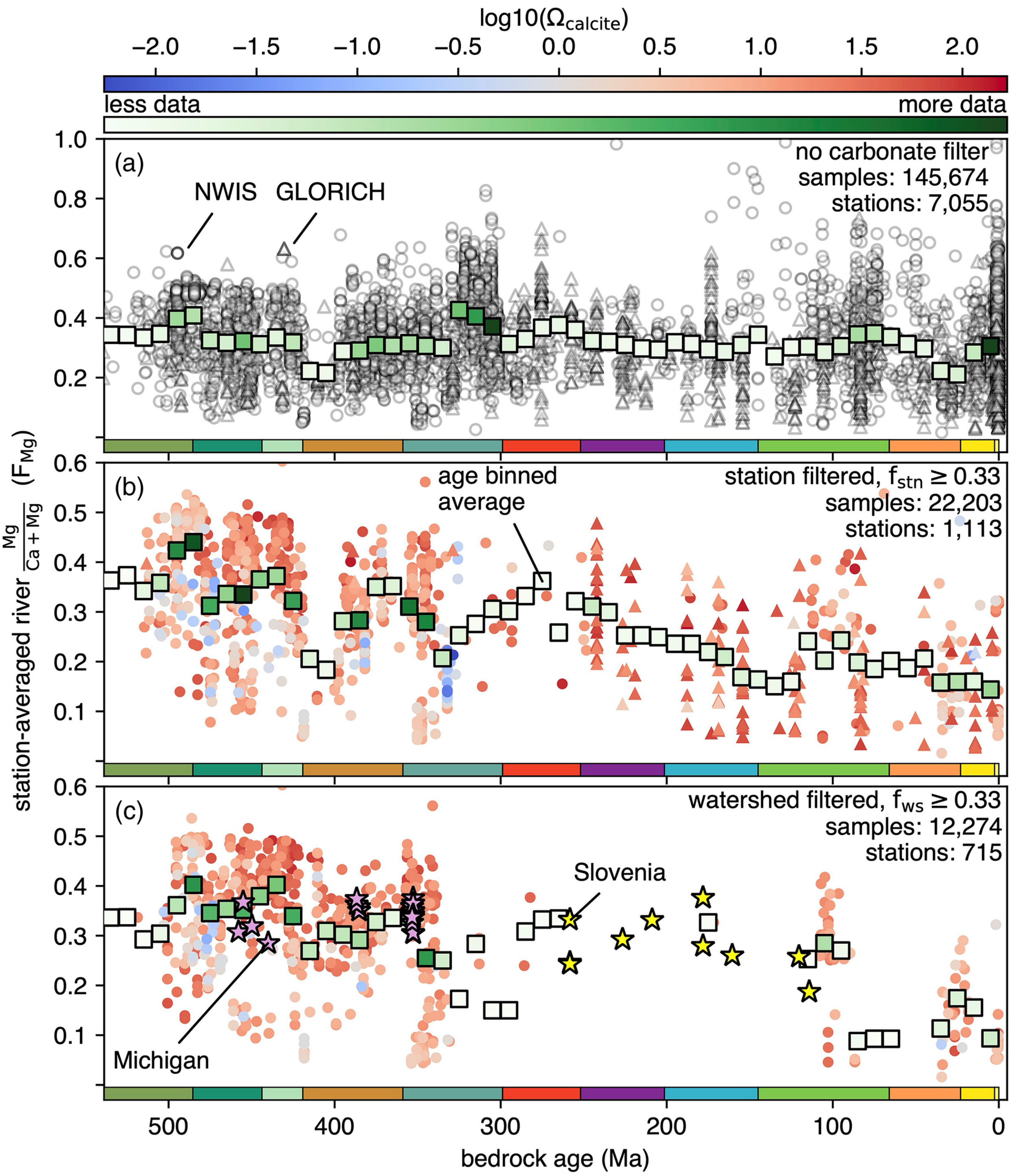

Figure 2 Station-averaged river Mg/(Ca + Mg) ratios (F_{Mg}) *vs.* bedrock age from the NWIS (circles) and GLORICH (triangles) databases, and 10 Myr binned means (squares, colour coded by the amount of data averaged in each bin, scaled to each time series). In **(a)**, all rivers are included, whereas **(b)** and **(c)** only show rivers that drain carbonate bedrock, have relatively low Na and K, and have a ratio of HCO_3^- to (Mg^{2+} + Ca^{2+}) between 1 and 2 (see Results). In **(b)**, f_{stn} value is used to filter for carbonate containing bedrock, and in **(c)**, f_{ws} is used. In **(b)** and **(c)**, values of F_{Mg} are colour coded by station-averaged calcite saturation (Ω; see Discussion). Also plotted in **(c)** are F_{Mg} from rivers in Michigan (purple stars; Williams *et al.*, 2007) and Slovenia (yellow stars; Szramek *et al.*, 2011) that drain carbonate dominated catchments, which are not included in the age binned averages.

for the coupled Ca-Mg-C-cycles in seawater (Arvidson *et al.*, 2011). First, it is generally thought that the Mg/Ca of seawater has oscillated over the Phanerozoic on a 100 Myr timescale with no long term secular change (*e.g.*, Lowenstein *et al.*, 2001; Weldeghebriel *et al.*, 2022), and it has been suggested that this might have been controlled by variations in the fraction of dolomite buried (*e.g.*, Holland *et al.*, 1996). However, there is no simple relationship between the dolomite/calcite ratio in carbonates and seawater Mg/Ca, suggesting that if the proposed oscillations in seawater Mg/Ca are correct, these were not driven by changes in the fraction of dolomite buried on continental shelves.

Second, the change in the fraction of dolomite as a function of carbonate sediment age means that carbonate weathering must be a source of Mg, and sink of Ca, from seawater, assuming the alkalinity released by carbonate weathering has been

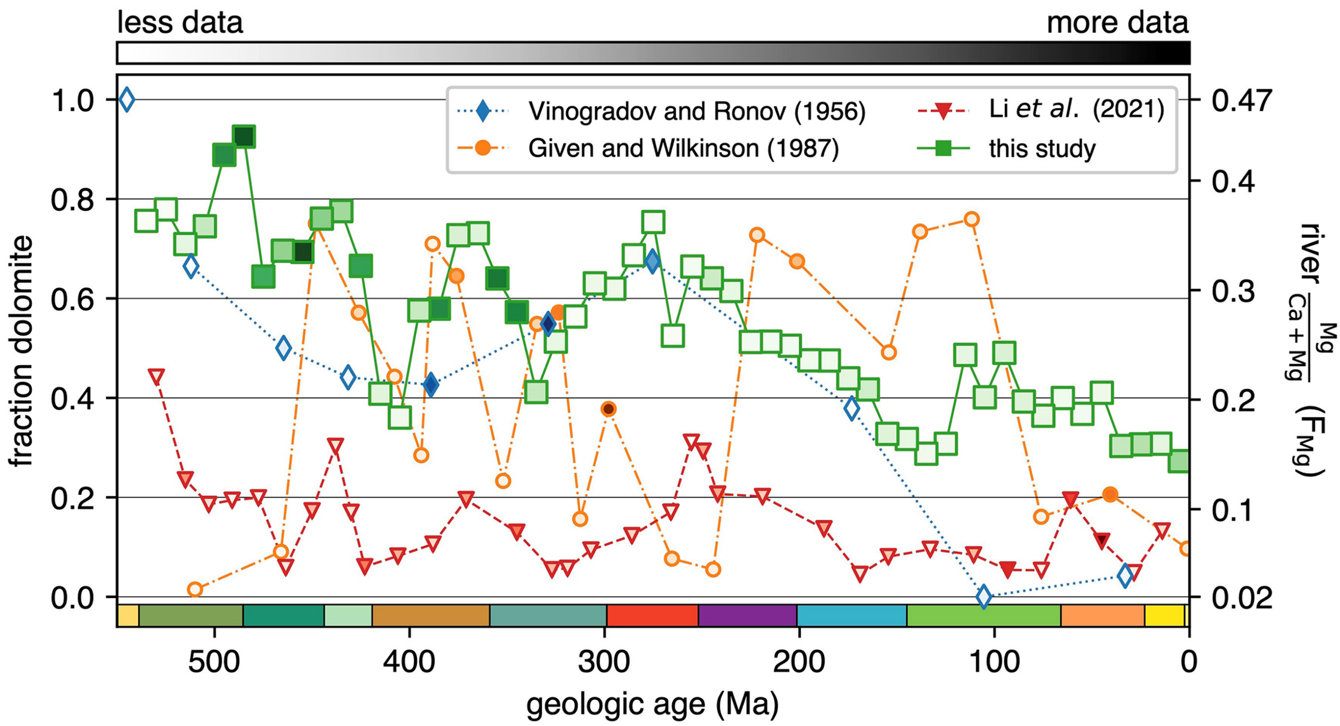

Figure 3 Using the age binned values from Figure 2b, river F_{Mg} (right y axis) is used to predict mole fraction dolomite in carbonate bedrock (left axis; see Discussion), and plotted *vs.* bedrock age. Fraction dolomite based on rock sample geochemistry from the Russian platform (Vinogradov and Ronov, 1956) and North America (Given and Wilkinson, 1987) and on a compilation of unit thicknesses of dolostones and limestones in carbonate sequences (Li *et al.*, 2021) are also shown. All records are colour coded by the relative amount of data averaged into each point, scaled to each time series.

consumed by carbonate precipitation. For example, given a rate of change in the Mg/(Ca + Mg) of continental carbonates of ~0.04 *per* 100 Myr (Fig. 3), and a half-life of carbonates in the continental crust of ~250 Myr (Wilkinson and Walker, 1989), the average carbonate precipitated has a Mg/(Ca + Mg) ~0.1 lower than the average carbonate dissolved during contemporaneous weathering. If carbonate weathering feeds 50 % of the ~20 Tmol yr^{-1} of carbonate burial (Wilkinson and Walker, 1989), a very conservative estimate, carbonate weathering is equivalent to a flux of 1 Tmol yr^{-1} of Mg into seawater. This suggestion should be testable using the Mg isotopic composition of seawater, given the strong fractionation of Mg isotopes between dolomite and Mg silicates, once robust records of the evolution of the Mg isotopic composition of seawater for the entire Phanerozoic are available.

The nature of the sink(s) for the Mg flux from dolomite weathering has important implications for the carbon cycle. The most likely sink is clay uptake, either in oceanic crust or in sediments. In the first scenario, the Mg released by dolomite dissolution may be largely exchanged for Ca in high or low temperature hydrothermal systems on the seafloor. In this model, the Ca could then be precipitated out of the ocean with the carbon released by dolomite dissolution as calcite, thus roughly balancing the carbon/alkalinity cycle. Alternatively, Garrels and Berner (1983) suggested that the net effect of dolomite dissolution and calcite precipitation is CO_2 release, through reactions such as:

$$H_2O + 6(Ca_{0.5}Mg_{0.5})CO_3 + 4SiO_2 \rightleftharpoons 3CaCO_3 + Mg_3Si_4O_{10}(OH)_2 + 3CO_2$$

in which Mg released by dolomite weathering reacts with Si to form authigenic Mg phyllosilicates, and the carbon released by dolomite weathering remains in the ocean-atmosphere system. Based on the Mg flux estimates given above, dolomite weathering could lead to the release of 1 Tmol yr^{-1} of CO_2 into the ocean-atmosphere system, which is equivalent to 10–25 % of solid Earth degassing (*e.g.*, Berner, 2004). While both sinks for the Mg released by dolomite weathering may have been important over the Phanerozoic, the potential for this process to play a non-trivial role in the global carbon cycle deserves further consideration.

Acknowledgements

We would like to thank two anonymous reviewers, whose comments improved the manuscript, and Gavin Foster for his work as editor.

Editor: Gavin Foster

Additional Information

Supplementary Information accompanies this letter at https://www.geochemicalperspectivesletters.org/article2316.

Cite this letter as: Husson, J.M., Coogan, L.A. (2023) River chemistry reveals a large decrease in dolomite abundance across the Phanerozoic. *Geochem. Persp. Let.* 26, 1–6. https://doi.org/10.7185/geochemlet.2316

References

Arvidson, R.S., Guidry, M.W., Mackenzie, F.T. (2011) Dolomite controls on Phanerozoic seawater chemistry. *Aquatic Geochemistry* 17, 735–747. https://doi.org/10.1007/s10498-011-9130-7

Berner, R.A. (2004) *The Phanerozoic Carbon Cycle*. Oxford University Press, New York.

Daly, R.A. (1909) First calcareous fossils and the evolution of the limestones. *Geological Society of America Bulletin* 20, 153–170. https://doi.org/10.1130/GSAB-20-153

Gaillardet, J., Dupré, B., Louvat, P., Allegre, C. (1999) Global silicate weathering and CO_2 consumption rates deduced from the chemistry of large rivers. *Chemical Geology* 159, 3–30. https://doi.org/10.1016/S0009-2541(99)00031-5

Garrels, R.M., Berner, R.A. (1983) The Global Carbonate-Silicate Sedimentary System — Some Feedback Relations. In: Westbroek, P., de Jong, E.W. (Eds.) *Biomineralization and Biological Metal Accumulation: Biological and Geological Perspectives*. Springer, Netherlands, 73–87.

Given, R.K., Wilkinson, B.H. (1987) Dolomite abundance and stratigraphic age; constraints on rates and mechanisms of Phanerozoic dolostone formation. *Journal of Sedimentary Research* 57, 1068–1078. https://doi.org/10.1306/212F8CF1-2B24-11D7-8648000102C1865D

Hartmann, J., Moosdorf, N. (2012) The new global lithological map database GLiM: A representation of rock properties at the Earth surface. *Geochemistry, Geophysics, Geosystems* 13, Q12004. https://doi.org/10.1029/2012GC004370

Hartmann, J., Lauerwald, R., Moosdorf, N. (2014) A brief overview of the GLObal RIver CHemistry Database, GLORICH. *Procedia Earth and Planetary Science* 10, 23–27. https://doi.org/10.1016/j.proeps.2014.08.005

Holland, H.D., Horita, J., Seyfried, W.E. (1996) On the secular variations in the composition of Phanerozoic marine potash evaporites. *Geology* 24, 993–996. https://doi.org/10.1130/0091-7613(1996)024<0993:OTSVIT>2.3.CO;2

Holland, H.D., Zimmermann, H. (2000) The dolomite problem revisited. *International Geology Review* 42, 481–490. https://doi.org/10.1080/00206810009465093

Humphreys, M.P., Lewis, E.R., Sharp, J.D., Pierrot, D. (2022) PyCO2SYS v1.8: marine carbonate system calculations in Python. *Geoscientific Model Development* 15, 15–43. https://doi.org/10.5194/gmd-15-15-2022

Land, L.S. (1998) Failure to Precipitate Dolomite at 25 °C from Dilute Solution Despite 1000-Fold Oversaturation after 32 Years. *Aquatic Geochemistry* 4, 361–368. https://doi.org/10.1023/A:1009688315854

Li, M., Wignall, P.B., Dai, X., Hu, M., Song, H. (2021) Phanerozoic variation in dolomite abundance linked to oceanic anoxia. *Geology* 49, 698–702. https://doi.org/10.1130/G48502.1

Lowenstein, T.K., Timofeeff, M.N., Brennan, S.T., Hardie, L.A., Demicco, R.V (2001) Oscillations in Phanerozoic seawater chemistry: evidence from fluid inclusions. *Science* 294, 1086–1088. https://doi.org/10.1126/science.1064280

Manche, C.J., Kaczmarek, S.E. (2021) A global study of dolomite stoichiometry and cation ordering through the Phanerozoic. *Journal of Sedimentary Research* 91, 520–546. https://doi.org/10.2110/jsr.2020.204

Morse, J.W., Mackenzie, F.T. (1990) *Geochemistry of Sedimentary Carbonates*. Developments in Sedimentology, 48, Elsevier, Amsterdam.

Peters, S.E., Husson, J.M., Czaplewski, J. (2018) Macrostrat: a platform for geological data integration and deep-time Earth crust research. *Geochemistry, Geophysics, Geosystems* 19, 1393–1409. https://doi.org/10.1029/2018GC007467

Petrash, D.A., Bialik, O.M., Bontognali, T.R., Vasconcelos, C., Roberts, J.A., McKenzie, J.A., Konhauser, K.O. (2017) Microbially catalyzed dolomite formation: From near-surface to burial. *Earth-Science Reviews* 171, 558–582. https://doi.org/10.1029/2018GC007467

Schmoker, J.W., Krystinik, K.B., Halley, R.B. (1985) Selected characteristics of limestone and dolomite reservoirs in the United States. *AAPG Bulletin* 69, 733–741. https://doi.org/10.1306/AD4627F9-16F7-11D7-8645000102C1865D

Szramek, K., Walter, L.M., Kanduc, T., Ogrinc, N. (2011) Dolomite versus calcite weathering in hydrogeochemically diverse watersheds established on bedded carbonates (Sava and Soča Rivers, Slovenia). *Aquatic Geochemistry* 17, 357–396. https://doi.org/10.1007/s10498-011-9125-4

Vinogradov, A., Ronov, A. (1956) Compositions of the sedimentary rocks of the Russian Platform in relation to the history of its tectonic movements. *Geokhimiya* 6, 533–559.

Weldeghebriel, M.F., Lowenstein, T.K., García-Veigas, J., Cendón, D.I. (2022) [Ca^{2+}] and [SO_4^{2-}] in Phanerozoic and terminal Proterozoic seawater from fluid inclusions in halite: The significance of Ca-SO_4 crossover points. *Earth and Planetary Science Letters* 594, 117–712. https://doi.org/10.1016/j.epsl.2022.117712

Wilkinson, B.H., Walker, J.C. (1989) Phanerozoic cycling of sedimentary carbonate. *American Journal of Science* 289, 525–548. https://doi.org/10.2475/ajs.289.4.525

Williams, E.L., Szramek, K.J., Jin, L., Ku, T.C., Walter, L.M. (2007) The carbonate system geochemistry of shallow groundwater–surface water systems in temperate glaciated watersheds (Michigan, USA): Significance of open-system dolomite weathering. *Geological Society of America Bulletin* 119, 515–528. https://doi.org/10.1130/B25967.1